2002

Histidinyl Radical Formation in the Self-peroxidation Reaction of Bovine Copper-Zinc Superoxide Dismutase

Michael R. Gunther

J. Andrew Peters

Meena K. Sivaneri

THE JOURNAL OF BIOLOGICAL CHEMISTRY
Vol. 277, No. 11, Issue of March 15, pp. 9160–9166, 2002

Printed in U.S.A.

Histidinyl Radical Formation in the Self-peroxidation Reaction of Bovine Copper-Zinc Superoxide Dismutase*

Received for publication, August 1, 2001, and in revised form, November 29, 2001
Published, JBC Papers in Press, January 2, 2002, DOI 10.1074/jbc.M107342200

Michael R. Gunther‡, J. Andrew Peters, and Meena K. Sivaneri

From the Department of Biochemistry and Molecular Pharmacology, West Virginia University, Morgantown, West Virginia 26506

In the absence of suitable oxidizable substrates, the peroxidase reaction of copper-zinc superoxide dismutase (SOD) oxidizes SOD itself, ultimately resulting in its inactivation. A SOD-centered free radical adduct of 2-methyl-2-nitrosopropane (MNP) was detected upon incubation of SOD with the spin trap and a hydroperoxide (either H_2O_2 or peracetic acid). Proteolysis by Pronase converted the anisotropic electron paramagnetic resonance (EPR) spectrum of MNP/•SOD to a nearly isotropic spectrum with resolved hyperfine couplings to several atoms with non-zero nuclear spin. Authentic histidinyl radical (from histidine + HO•) formed a MNP adduct with a very similar EPR spectrum to that of the Pronase-treated MNP/•SOD, suggesting that the latter was centered on a histidine residue. An additional hyperfine coupling was detected when histidine specifically ^{13}C-labeled at C-2 of the imidazole ring was used, providing evidence for trapping at that atom. All of the experimental spectra were convincingly simulated assuming hyperfine couplings to 2 nearly equivalent nitrogen atoms and 2 different protons, also consistent with trapping at C-2 of the imidazole ring. Free histidinyl radical consumed oxygen, implying peroxyl radical formation. MNP-inhibitable oxygen consumption was also observed when cuprous SOD but not cupric SOD was added to a H_2O_2 solution. Formation of 2-oxohistidine, the stable product of the SOD-hydroperoxide reaction, required oxygen and was inhibited by MNP. These results support formation of a transient SOD-peroxyl radical.

Copper-zinc superoxide dismutase (SOD)[1] is the primary cytosolic superoxide detoxification enzyme in eukaryotes. The enzymatic disproportionation of superoxide produces molecular oxygen and hydrogen peroxide. Under normal conditions, hydrogen peroxide is further detoxified through its reaction with either catalase or glutathione peroxidase. In addition to its normal reaction with superoxide, SOD has also been shown to react with the hydrogen peroxide product of its catalytic cycle, ultimately leading to the inactivation of the SOD (1, 2). In addition to the inactivation of SOD, the latter (peroxidase) activity has also been shown to oxidize substrates (3, 4).

The peroxidase activity of SOD has been proposed to contribute to the toxicity associated with the mutant forms of SOD that cause some cases of familial amyotrophic lateral sclerosis (fALS) (5–7). In support of that hypothesis, a higher intracellular concentration of H_2O_2 has been measured in lymphoblast cell lines derived from fALS patients compared with cell lines from control patients (8). Increased oxidative damage to proteins has been detected in transgenic mice expressing a fALS-associated mutant human SOD (9–10), supporting the possibility that oxidation of SOD and/or other cellular proteins may contribute to the development of the disease.

The normal enzymatic reaction mechanism of SOD involves the alternating reduction and oxidation of the active site copper ion (Reactions 1–2).

$$\text{SOD-Cu}^{2+} + O_2^- \rightarrow \text{SOD-Cu}^{+} + O_2$$

REACTION 1

$$\text{SOD-Cu}^{+} + O_2^- + 2H^+ \rightarrow \text{SOD-Cu}^{2+} + H_2O_2$$

REACTION 2

The peroxidase reaction of SOD involves the reaction between the cuprous SOD intermediate formed in Reaction 1 above with H_2O_2. The SOD product of that reaction is highly oxidizing and has been alternately described as hydroxyl radical (free or bound to the active site cupric ion), or as some highly oxidizing hypervalent copper species (Reaction 3) (11).

$$\text{SOD-Cu}^{+} + H_2O_2 \rightarrow \text{SOD-Cu}^{2+} - \cdot\text{OH or SOD-Cu}^{3+} = O + H^+$$

REACTION 3

That intermediate can oxidize substrates directly or by way of its reaction with bicarbonate ions to form an intermediate carbonate radical, which subsequently oxidizes other substrates (2–4). The H_2O_2-reactive cuprous SOD can be produced either by oxidation of H_2O_2 by the active site cupric ion (Reaction 4) or by reduction of the cupric ion by cellular reductants (11).

$$\text{SOD-Cu}^{2+} + H_2O_2 \rightarrow \text{SOD-Cu}^{+} + HO_2^{\cdot} + H^+$$

REACTION 4

In the absence of a suitable substrate, the SOD itself can be oxidized, resulting in damage to one or more amino acid residues of the enzyme (1, 12). Although the stable product of the self-peroxidation of bovine SOD is 2-oxohistidine formed by the oxidation of a histidine residue (His-118) (12), the mechanism by which histidine is converted to the final product has not been determined (13). It is also unclear whether any other

* This work was supported by a grant from the ALS Association. The costs of publication of this article were defrayed in part by the payment of page charges. This article must therefore be hereby marked "*advertisement*" in accordance with 18 U.S.C. Section 1734 solely to indicate this fact.

‡ To whom correspondence should be addressed: Dept. of Biochemistry and Molecular Pharmacology, West Virginia University, P.O. Box 9142, Morgantown, WV 26506. Tel.: 304-293-0714; E-mail: mgunther@hsc.wvu.edu.

[1] The abbreviations used are: SOD, copper-zinc superoxide dismutase; MNP, 2-methyl-2-nitrosopropane; EPR, electron paramagnetic resonance; MNP/•His, the histidinyl radical adduct of MNP; MNP/•SOD, the SOD radical adduct of MNP; fALS, familial amyotrophic lateral sclerosis; DTPA, diethylenetriaminepentaacetic acid.

amino acid residues are also oxidized.

In the present study, the nature of the amino acid residue of bovine SOD that is oxidized in the self-peroxidation reaction was determined and its chemistry was explored. Electron paramagnetic resonance (EPR) spectroscopy and the spin trapping technique were applied toward identification of the amino acid residue oxidized in the peroxidase reaction. The possible reaction of the product radical with oxygen was studied using an oxygen electrode and UV-visible spectroscopy.

MATERIALS AND METHODS

Bovine SOD and Pronase were purchased from Roche Molecular Biopharmaceuticals (Indianapolis, IN). 2-Methyl-2-nitrosopropane (MNP), peracetic acid, diethylpyrocarbonate, titanium (III) chloride, and histidine hydrochloride were from Aldrich (Milwaukee, WI). Diethylenetriaminepentaacetic acid (DTPA) and *t*-butylhydroperoxide were from Sigma. Ferrous sulfate and hydrogen peroxide were from Fisher Scientific (Pittsburgh, PA).

Stock Solutions—Stock solutions of SOD were prepared by dissolving the lyophilized protein into 50 mM sodium phosphate buffer, pH 7.4. The SOD concentrations of the stock solutions (typically 1–2 mM, depending on the experiment to be performed) were determined by atomic absorbance spectroscopy using a PerkinElmer model 380 atomic absorbance spectrophotometer. The EPR spectra of the SOD solutions provided no evidence for free copper ions (data not shown). SOD solutions enriched in the cuprous form of the enzyme were prepared by addition of cysteine at the same concentration as the copper to SOD stock solutions prepared in argon-saturated phosphate buffer followed by a 10-min incubation at 30 °C. Stock solutions (100 mM) of H_2O_2, peracetic acid, and *t*-butylhydroperoxide were prepared by dilution of the concentrated solutions into E-pure deionized water. Stock solutions of MNP (22 mM) were prepared in 50 mM sodium phosphate buffer, pH 7.4, by stirring overnight in a sealed, foil-covered flask. When MNP was added at late time points, it was prepared as a 1 M solution in argon-saturated acetonitrile and stored in the dark at 4 °C until use. Stock solutions of DTPA were prepared as the trisodium salt at a concentration of 100 mM in deionized water. Stock solutions of ferrous sulfate were prepared in deionized water at a concentration of 100 mM.

Spin-trapping Experiments—Incubations contained SOD (250 or 500 μM), DTPA (1 mM) to prevent any reactions of trace transition metal ions or released copper ions, and the spin trap MNP (11 to 16 mM). Reactions were initiated by addition of H_2O_2, peracetic acid, or *t*-butylhydroperoxide (final concentration 1 or 2 mM, depending on SOD concentration) to solutions containing the spin trap and SOD. Reactions involving cuprous SOD were initiated by addition of the SOD to solutions containing MNP, DTPA, and the hydroperoxide used. Hydrolyzed MNP/SOD adducts were obtained by treatment with Pronase (20 mg/ml) for 5 min at 30 °C prior to the acquisition of their EPR spectra. Reactions involving histidine were initiated by addition of ferrous sulfate (1 mM) to a mixture containing histidine (20 mM), H_2O_2 (2 mM), and MNP (16 mM) in deionized water. EPR spectra were obtained using a Bruker EMX EPR spectrometer equipped with a SHQ resonator after the solutions were transferred into a flat EPR sample cell (Wilmad Glass Co., Buena, NJ). EPR spectrometer settings used for each experiment are reported in the figure legends. Computer simulations of EPR spectra were calculated using the WinSim program in the NIEHS public ESR software tools package (www.epr.niehs.nih.gov/) (14).

Direct EPR Spectroscopy—H_2O_2 (2–8 mM, depending upon [SOD]) was added to a solution containing SOD (0.5–1 mM Cu) and DTPA (2 mM). After mixing with a vortex mixer, the samples were drawn into a truncated disposable 1-ml plastic syringe and frozen in liquid nitrogen, typically within 7 s of the addition of H_2O_2. After freezing the samples were transferred to a quartz fingertip Dewar containing liquid nitrogen and their EPR spectra were obtained using a Bruker EMX spectrometer. The following instrument parameters were used: modulation amplitude, 4 G; time constant, 1.3 s; scan time 335 s/300 G; receiver gain, 5×10^3; the microwave power was systematically varied; 8 scans were averaged to obtain the final spectra. Integrated spectral intensities were obtained using the EPR-main program of the NIEH public EPR software tools package (www.epr.niehs.nih.gov/).

Oxygen Concentration Determinations—The oxygen concentrations in solutions of SOD or histidine were followed as a function of time using a YSI Model 5300 Biological Oxygen monitor (Yellow Springs Instrument Co., Yellow Springs, OH) equipped with a Clark electrode. Reactions were initiated by addition of the final component (ferrous sulfate in the case of histidine reactions, SOD in the case of SOD reactions) after establishment of a steady baseline oxygen concentration. In histidine experiments, the solutions contained histidine (20 mM), H_2O_2 (1 or 2 mM), and ferrous sulfate (0.5 or 1 mM). SOD experiments contained SOD (75 μM), DTPA (100 μM), and H_2O_2 (250 μM). When MNP was used the histidine or the H_2O_2 and DTPA (in the SOD reactions) were dissolved in MNP stock solution (22 mM). Experiments were repeated at least 3 times to ensure reproducibility.

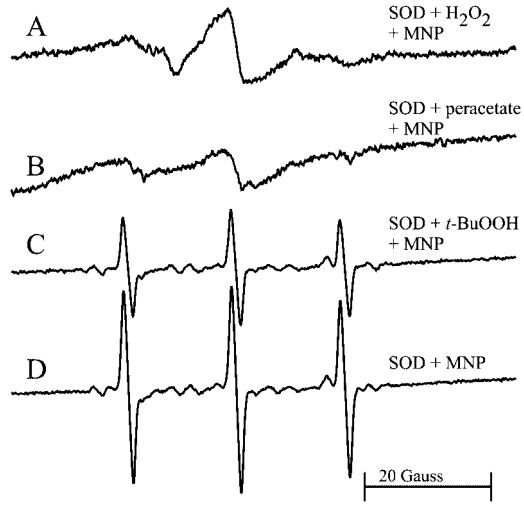

FIG. 1. **EPR spectra from the spin trapping of the product of the reaction between SOD and hydroperoxides.** *A*, H_2O_2 (2 mM) was added to a solution containing SOD (0.5 mM) and MNP (16.5 mM). *B*, peracetic acid (PAA) (2 mM) was added to a solution containing SOD (0.5 mM) and MNP (16.5 mM). *C*, *t*-butylhydroperoxide (2 mM) was added to a solution containing SOD (0.5 mM) and MNP (16.5 mM). *D*, the EPR spectrum obtained from a solution containing SOD (0.5 mM) and MNP (16.5 mM) with no added hydroperoxide. All spectra were acquired using the following instrument settings: modulation amplitude, 2 G; time constant, 1.3 s; scan time, 1342 s (80 G); receiver gain, 5×10^5; microwave power, 20 mW.

UV-visible Spectroscopy—The formation of the stable product of the oxidation of SOD by H_2O_2 was followed using UV-visible difference spectroscopy. The sealed quartz sample cuvette contained SOD (210 μM Cu) and H_2O_2 (5 mM) and was incubated at room temperature for the desired time before the difference spectrum was obtained. The sealed quartz reference cuvette contained SOD (210 μM). Difference spectra were obtained under air-saturated, argon-saturated, and oxygen-saturated conditions. The effects of MNP on the observed difference spectra were determined by adding MNP to a final concentration of 20 mM in both sample and reference cuvettes from a stock solution (1 M) prepared in acetonitrile. UV-visible spectra were collected using an Aminco DW-2000 spectrophotometer operating in split (sample and reference) mode.

Diethylpyrocarbonate Treatment—Treatment of proteins with diethylpyrocarbonate results in the *N*-ethoxylcarbonylation of histidine residues on the protein (15). SOD was incubated with a 16-fold molar excess of diethylpyrocarbonate (SOD has 8 histidine residues per subunit) for 10 min at 37 °C. After the incubation, an aliquot of the SOD solution was removed and diluted 1:100 into water and its UV-visible spectrum was obtained from 220 to 400 nm. The difference in absorbance of the diethylpyrocarbonate-treated SOD and untreated SOD at 240 nm was used to calculate the number of histidine residues modified per subunit using a molar extinction coefficient of 3,600 M^{-1} cm^{-1} (15).

RESULTS

To determine whether a SOD-centered free radical is formed during its H_2O_2-induced inactivation, bovine SOD was incubated with H_2O_2 and the spin trap MNP. The EPR spectrum of the SOD/H_2O_2/MNP reaction mixture was anisotropic and typical of an immobilized nitroxide-free radical adduct (Fig. 1*A*). Protein radicals spin trapped with MNP typically give an immobilized nitroxide EPR spectrum due to the proximity of the radical center (the N-O bond) to the protein, which limits the rotational dynamics of the nitroxide-free radical. To determine whether the SOD-centered free radical adduct formation was H_2O_2-specific, the experiment was repeated using the organic hydroperoxides peracetate and *t*-butylhydroperoxide (Fig. 1, *B*

and *C*). When peracetate was used, a weak immobilized nitroxide spectrum on the side of a copper line was observed (Fig. 1*B*). The copper spectrum likely arose from the release of some copper from the SOD active site by the acidic peracetate solution. When a higher buffer concentration was used, the slope of the baseline was greatly decreased (data not shown).

When *t*-butylhydroperoxide was substituted for H_2O_2 in the reaction mixture, the anisotropic EPR spectrum was replaced by an isotropic, 3-line signal with $a^N = 17.2$ G, characteristic of di-*t*-butylnitroxide (Fig. 1*C*). The spectrum of di-*t*-butylnitroxide was also detected when no hydroperoxide was added to the reaction mixture (Fig. 1*D*). Di-*t*-butylnitroxide is a contaminant frequently found in solutions of MNP (16). The failure to observe the contaminant di-*t*-butylnitroxide in the reaction mixtures containing either H_2O_2 or peracetate indicates that the peroxidase activity of SOD is able to oxidize the di-*t*-butylnitroxide to form EPR-silent product(s). The detection of di-*t*-butylnitroxide when *t*-butylhydroperoxide was included in the reaction mixtures is likely due to the inability of SOD to utilize the hydroperoxide to initiate its peroxidase reaction.

The proposed mechanism for the peroxidase reaction of SOD involves the reaction between cuprous SOD and the hydroperoxide to form the product-free radical(s) (reaction 3 above). According to that mechanism, enrichment of the SOD solution with the cuprous form of the enzyme should promote SOD-centered radical formation. When cuprous SOD was reacted with H_2O_2, the intensity of the detected EPR spectrum was increased by about 2-fold, compared with an equal concentration of cupric SOD (data not shown). Similarly, the intensity of the detected EPR spectrum was increased by about 3-fold when cuprous SOD was reacted with peracetate compared with the same concentration of cupric SOD (data not shown).

An intact active site copper center is required for the proposed peroxidase mechanism to be involved in SOD-centered free radical formation. Inclusion of 1 mM sodium cyanide, a well known inhibitor of SOD activity (17), in the reaction mixture resulted in the detection of the EPR spectrum of di-*tert*-butylnitroxide (data not shown), indicating that SOD-centered free radical formation was inhibited by cyanide. Heat denaturation of the SOD at 100 °C for 1 h (18, 19) also prevented SOD-centered radical formation (data not shown), further confirming that an intact copper center is required for the reaction. To further control for possible reactions of non-active site copper, all of the reaction mixtures in this study contained the chelator DTPA at a concentration that exceeded that of the copper. DTPA has previously been shown to prevent hydroxyl radical formation from the reaction between Cu^+ and H_2O_2 (20).

The anisotropic nature of the EPR spectra obtained from products of the reactions between SOD and either H_2O_2 or peracetate prevent the detection of hyperfine couplings from atoms of the original radical that would allow an assignment of the spectrum to a particular amino acid radical. Treatment of the solution with the nonspecific protease mixture Pronase prior to acquisition of the EPR spectra of the solutions resulted in the conversion of the anisotropic spectrum to a nearly isotropic spectrum with reasonably well resolved hyperfine couplings (Fig. 2*A*). When the reaction mixture containing cuprous SOD, peracetate, and MNP was treated with Pronase, an identical EPR spectrum to that shown in Fig. 2*A* was detected, consistent with the same amino acid residue being oxidized in both cases (Fig. 2*B*). Both experimental spectra exhibited complex hyperfine structures (Fig. 2, *A* and *B*), suggesting couplings to more than one hydrogen and/or nitrogen atom(s).

The complexity of the hyperfine coupling patterns in the EPR spectra of Pronase-treated SOD suggested that the oxidized amino acid residue might be a histidine. A strikingly similar

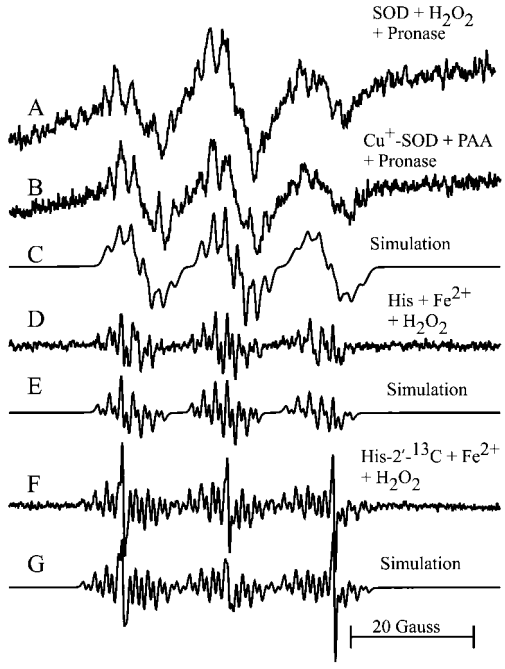

FIG. 2. **EPR spectra acquired after Pronase treatment of SOD/·MNP adducts.** *A*, SOD (0.5 mM) was incubated with H_2O_2 (2 mM) and MNP (16.5 mM). Pronase (20 mg/ml) was added after H_2O_2 and the EPR spectrum was acquired after a 5-min incubation at 30 °C. *B*, cuprous SOD (0.25 mM) was incubated with peracetic acid (0.5 mM) and MNP (16.5 mM). Pronase (20 mg/ml) was added and the EPR spectrum was acquired after a 10-min incubation at 30 °C. *C*, computer simulation of spectrum B calculated using the following hyperfine coupling constants: $a^{N(NO)} = 15.3$ G; $a^N = 1.85$ G; $a^N = 1.9$ G; $a^H = 2.1$ G; $a^H = 0.88$ G. The WinSim program was allowed to vary the linewidth for each line from the primary nitroxide to provide the best fit. *D*, EPR spectrum acquired from an incubation containing histidine (80 mM), MNP (16.5 mM), H_2O_2 (2 mM), and Fe^{2+} (1 mM). *E*, computer simulation of spectrum D calculated using the following hyperfine coupling constants: $a^{N(NO)} = 15.3$ G; $a^N = 1.85$ G; $a^N = 1.89$ G; $a^H = 2.1$ G, and $a^H = 0.8$ G. The program was allowed to adjust the linewidths for each line from the primary nitroxide to provide the best fit to the experimental data. The spectrum of di-*t*-butylnitroxide ($a^N = 17.2$ G) was included in the simulation at a relative concentration of 3% of the total signal to obtain a better fit to the experimental spectrum. *F*, the EPR spectrum acquired from a solution containing histidine labeled specifically at C-2 of the indole ring with ^{13}C (80 mM), H_2O_2 (4 mM), and Fe^{2+} (2 mM). *G*, computer simulation of experimental spectrum F, calculated using the following hyperfine coupling constants: $a^{N(NO)} = 15.3$ G; $a^N = 1.85$ G; $a^N = 1.89$ G; $a^H = 2.11$ G; $a^H = 0.8$ G; and $a^{13C} = 4.85$ G. A lower concentration of di-*t*-butylnitroxide (~1% of total intensity) was included in the calculated spectrum. Spectrum A was acquired using a modulation amplitude of 1 G, a time constant of 2.6 s, a scan time of 1342 s (80 G), a receiver gain of 5×10^5, and a microwave power of 20 mW. Four scans were added together to obtain the final spectrum. Spectrum B was acquired using the same parameters as Spectrum A, but only one scan was collected. Spectra D and F were acquired using the following instrument parameters: modulation amplitude, 0.7 G; time constant, 1.3 s; scan time, 1342 s (80 G); receiver gain, 5×10^5; microwave power, 20 mW.

EPR spectrum was detected when a solution of histidine (20 mM) was incubated with the Fenton reagent ($Fe^{2+} + H_2O_2$) and MNP (Fig. 2*D*). Coordination of the ferrous iron by the imidazole ring of histidine might promote oxidation at a particular atom on the imidazole ring. To control for that, Ti^{3+}, which does not appear to be coordinated by imidazole (21), was used in place of iron, with very similar results (data not shown). When the experiment was repeated in D_2O, a nearly identical EPR spectrum was obtained (data not shown), indicating that none of the resolved hyperfine couplings came from exchangeable hydrogen atoms. When the experiment was repeated using histidine specifically ^{13}C-labeled at C-2 of the imidazole ring of histidine (see Fig. 9 for the ring numbering system), a

splitting in the EPR spectrum was detected with $a^{^{13}C} = 4.85$ G, providing strong evidence for adduct formation at that carbon atom (Fig. 2*F*).

To assist in the deconvolution of the hyperfine coupling pattern of the EPR spectrum of MNP/•His, a simulated EPR spectrum was calculated and compared with the experimental spectrum. The experimental spectrum was best matched by the simulated spectrum when the following hyperfine coupling constants were used: $a^N = 15.3$ G for the nitroxide nitrogen, $a^N = 1.8$ G and $a^N = 1.9$ G for the two imidazole nitrogens, and $a^H = 2.1$ G for an imidazole hydrogen atom, and $a^H = 0.8$ G for another imidazole proton (Fig. 2*E*). The EPR spectrum obtained from the Pronase-treated SOD sample was convincingly simulated using the same hyperfine coupling constants (Fig. 2*C*). Those results support the trapping of a histidinyl radical from SOD. The EPR spectrum of MNP/•His obtained in D_2O was computer simulated using the same parameters used for MNP/•His in H_2O with only a slight difference in the amount of di-*t*-butylnitroxide included in the calculated spectrum (data not shown).

In an attempt to confirm that the detected SOD-centered free radical adduct was formed at a histidine residue, the experiment was repeated using SOD pretreated with diethylpyrocarbonate, which labels the imidazole rings of histidine residues (15). Comparison of the UV-spectra of SOD incubated for 10 min at 37 °C with a 16-fold molar excess of diethylpyrocarbonate to that of untreated SOD indicated that approximately half of the histidine residues on the SOD were modified by the diethylpyrocarbonate treatment. When hydrogen peroxide and MNP were added to diethylpyrocarbonate-treated SOD, the intensity of the detected EPR spectrum was decreased by about 75% (spectra not shown). In addition, the apparent value of $a_{||}$ obtained from the immobilized nitroxide spectra increased from 18.1 G for the untreated SOD to 22.5 G for the treated SOD, indicating that a different amino acid residue radical had been trapped in the latter case. However, the radical adduct formed to the diethylpyrocarbonate-treated SOD was insufficiently stable to characterize after Pronase treatment (data not shown).

The reaction between SOD and H_2O_2 has been proposed to form 2-oxohistidine through the addition of a hydroxyl radical formed in the SOD active site to the imidazole ring of a histidine residue (12). Our detection of a histidinyl radical by spin trapping supports a free radical mechanism for the formation of 2-oxohistidine. In addition to the direct addition of HO• to a histidine residue, 2-oxohistidine could also be formed from histidinyl radical, either after addition of molecular oxygen to form a peroxyl radical or after the addition of water to histidinyl radical. If 2-oxohistidine formation involves intermediate histidinyl radical formation, trapping the precursor radical with a spin trap (MNP) should prevent its formation. Incubation of SOD with H_2O_2 resulted in the development of an absorbance band at ~295 nm, detected as the difference between the SOD-H_2O_2 incubation and SOD without added H_2O_2 (Fig. 3*A*), consistent with 2-oxohistidine formation (12). Formation of the absorbance band at 295 nm was prevented by inclusion of the spin trap MNP in the reaction mixture (Fig. 3*B*).

If 2-oxohistidine formation occurs through a peroxyl radical intermediate, its formation should also be prevented in the absence of molecular oxygen. When SOD was reacted with H_2O_2 in an argon-saturated solution, the UV spectrum featuring absorbance at 295 nm was replaced by a spectrum with absorbance bands at 250 and 280 nm (Fig. 4*A*). That spectrum is similar to the spectrum reported for the free radical formed in the reaction between histidine and aqueous electrons (22). The UV spectrum obtained after MNP was added to the anaerobic SOD-H_2O_2 solution consisted of a strong band at 328 nm with no absorbance between 250 and 300 nm (Fig. 4*B*). That result suggests that the product with strong absorbance between 250 and 300 nm is a compound that readily reacts with MNP, *i.e.* a free radical. When the experiment was repeated in oxygen-saturated buffer, the same UV spectrum was obtained as in the air-saturated experiment, but the final spectrum was obtained at an earlier time point (data not shown).

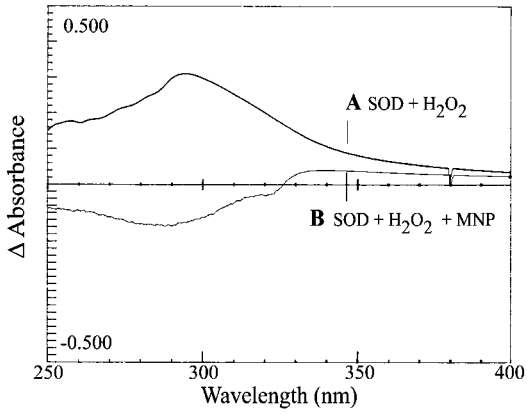

FIG. 3. **Changes in the UV spectrum of a solution of SOD upon reaction with H_2O_2 under air-saturated conditions.** *Trace A*, the difference spectrum between a solution containing SOD (210 μM Cu) and H_2O_2 (5 mM) incubated for 2.5 h at 30 °C and a solution containing SOD (210 μM Cu). *Trace B,* the difference spectrum between a solution containing SOD (210 μM Cu), H_2O_2 (5 mM), and MNP (22 mM) incubated for 2.5 h at 30 °C and a solution containing SOD (210 μM Cu) and MNP (22 mM).

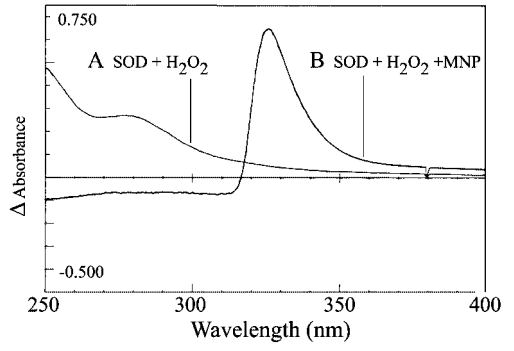

FIG. 4. **The UV spectrum of a reaction mixture containing SOD and H_2O_2 under anaerobic conditions.** *Trace A*, the difference spectrum between a solution containing SOD (200 μM Cu) and H_2O_2 (5 mM) incubated for 60 min at room temperature in argon-saturated buffer and a solution containing SOD (200 μM Cu) in argon-saturated buffer. *Trace B*, the difference spectrum obtained after MNP (20 mM) was added to the solutions in both sample and reference cuvettes used to obtain difference spectrum A.

To confirm that the addition of spin trap resulted in conversion of a histidinyl radical to a spin adduct, the EPR spectrum of a solution of SOD incubated with H_2O_2 under argon-saturated conditions was obtained after addition of MNP (Fig. 5*A*). The EPR spectrum of the anaerobic (argon-saturated) incubation was consistent with the formation of an immobilized nitroxide, *i.e.* a protein-centered radical was spin-trapped. Addition of MNP to an air-saturated solution of SOD and H_2O_2 after a 30-min incubation at room temperature resulted in detection of the EPR spectrum of di-*t*-butylnitroxide (Fig. 5*B*). Pronase treatment of the solution giving rise to spectrum 5A resulted in the detection of a spectrum that was very similar to spectrum 2A, confirming the trapping of a histidinyl radical (data not shown).

There are two possible explanations for the absence of the spectrum of the contaminant di-*t*-butylnitroxide in spectrum

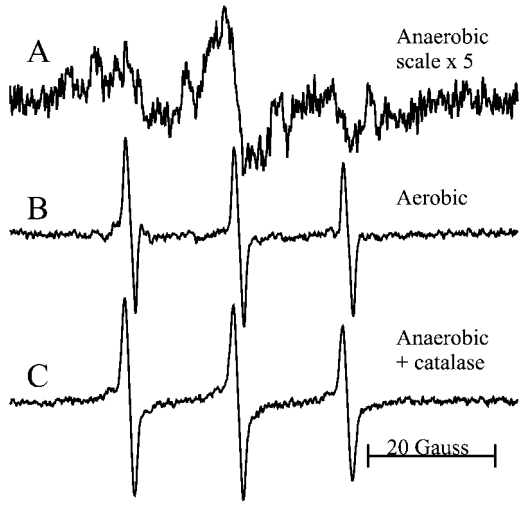

FIG. 5. **EPR spectra obtained when MNP was added to solutions containing SOD and H_2O_2 after a 30-min incubation.** *A*, MNP (20 mM) was added to an argon-saturated solution containing SOD (200 μM Cu) and H_2O_2 (2 mM) after a 30-min incubation. *B*, MNP (20 mM) was added to an air-saturated solution containing SOD (200 μM Cu) and H_2O_2 (2 mM) after a 30-min incubation. *C,* catalase (320 nM), then MNP (20 mM), were sequentially added to an argon-saturated solution containing SOD (200 mM Cu) and H_2O_2 (2 mM) incubated for 30 min at room temperature.

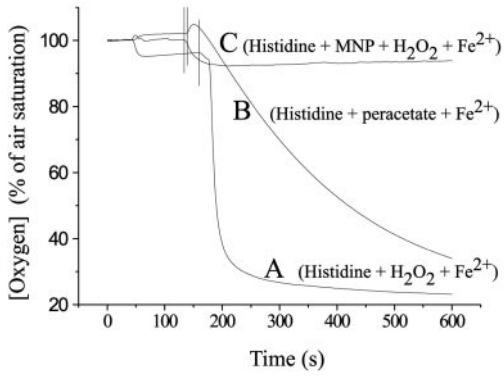

FIG. 6. **The reaction between histidine and hydroxyl radical results in the consumption of oxygen from the solution.** *Trace A*, changes in oxygen concentration when Fe^{2+} (1.0 mM) was added to a solution containing histidine (20 mM) and H_2O_2 (2 mM). *Trace B*, changes in oxygen concentration when Fe^{2+} (0.5 mM) was added to a solution containing histidine (20 mM) and peracetic acid (1 mM). *Trace C*, changes in oxygen concentration when Fe^{2+} (1 mM) was added to a solution containing histidine (20 mM), H_2O_2 (2 mM), and MNP (22 mM).

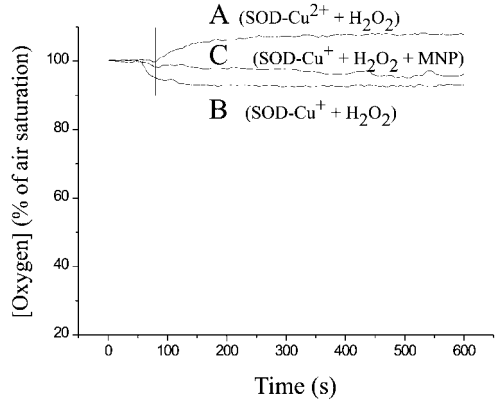

FIG. 7. **The histidinyl radical produced in the reaction between cuprous SOD and H_2O_2 consumes oxygen from the solution.** *Trace A*, changes in the oxygen concentration of a solution of H_2O_2 (250 μM) and DTPA (100 μM) after the addition of SOD (Cu^{2+}, 75 μM Cu). *Trace B*, changes in the oxygen concentration of a solution containing H_2O_2 (250 μM) and DTPA (100 μM) after the addition of SOD (Cu^{+}, 75 μM Cu). *Trace C*, changes in the oxygen concentration of a solution containing H_2O_2 (250 μM), DTPA (100 μM), and MNP (20 mM) after the addition of SOD (Cu^{+}, 75 μM Cu).

5A. Oxygen might be required for the H_2O_2-dependent loss of the peroxidase activity of SOD or the SOD-centered histidinyl radical might convert the di-*t*-butylnitroxide to EPR-silent product(s). To differentiate between the two possibilities, an anaerobic incubation of SOD and H_2O_2 was treated with catalase to remove any residual H_2O_2 prior to the addition of the spin trap. The EPR spectrum of that solution was the isotropic spectrum of di-*t*-butylnitroxide (Fig. 5*C*). Those data suggest that oxygen is involved in the decay of the histidinyl radical with subsequent loss of peroxidase activity, implying the formation of a peroxyl radical.

The ability of histidinyl radical to consume oxygen was determined using an oxygen electrode to assess the possibility of peroxyl radical formation. The reaction between histidine and hydroxyl radical (from either H_2O_2 or peracetic acid + Fe^{2+}) resulted in the rapid consumption of dissolved oxygen (Fig. 6, *A* and *B*). A similar result was observed when Ti^{3+} was substituted for Fe^{2+} in the incubation (data not shown), indicating that coordination of the metal ion by the imidazole ring was not necessary for oxygen consumption. Trapping of the histidinyl radical by inclusion of MNP in the reaction mixture prevented the consumption of oxygen in the solution (Fig. 6*C*). Those data confirm that histidinyl radical will react with molecular oxygen to form the corresponding peroxyl radical.

To determine whether the SOD-centered histidinyl radical will react with molecular oxygen to form a peroxyl radical, the effects of the addition of SOD to a solution containing H_2O_2 on the oxygen consumption were determined. Addition of 75 μM SOD to a solution containing 250 μM H_2O_2 resulted in an increase in the oxygen concentration in the solution (Fig. 7*A*). That result is reasonable since the initial reaction between SOD and H_2O_2 results in the formation of $HO_2^{\cdot}$ (Reaction 4 above), which disproportionates either spontaneously or catalyzed by SOD to form molecular oxygen and H_2O_2 (Reactions 1 and 2 above). Unfortunately, the oxygen release from the SOD reaction masks any oxygen consumption by the SOD-centered histidinyl radical that is formed in the subsequent reaction between cuprous SOD and another molecule of H_2O_2. When SOD that had been previously enriched in the cuprous form was added to a H_2O_2 solution, however, the oxygen concentration of the solution initially decreased followed by a leveling off (Fig. 7*B*). That result is consistent with the histidinyl radical reacting with O_2 to form the corresponding peroxyl radical and either subsequently being inactivated or having the oxygen production from the reaction observed between cupric SOD in Fig. 7*A* match the oxygen consumption by the histidinyl radical. The oxygen consumption observed when cuprous SOD was reacted with H_2O_2 was blunted by the inclusion of MNP in the reaction mixture (Fig. 7*C*), confirming that spin trapping the histidinyl radical prevents its reaction with O_2 to form a peroxyl radical.

The indirect evidence for the formation of a peroxyl radical intermediate from the reaction between SOD and H_2O_2 suggested that we might be able to directly detect a peroxyl radical by EPR spectroscopy. Because peroxyl radicals are not typically stable, they are frequently studied at low temperature, which decreases the rate of the reactions by which they decompose. When a mixture of SOD (1 mM Cu), DTPA (2 mM), and H_2O_2 (8 mM) was frozen in liquid nitrogen within 7 s of the addition of H_2O_2, the EPR spectrum detected at liquid nitrogen temperatures was dominated by the spectrum of the active site Cu^{2+} (Fig. 8*A*). A derivative-shaped line with a g value of 2.0045 was

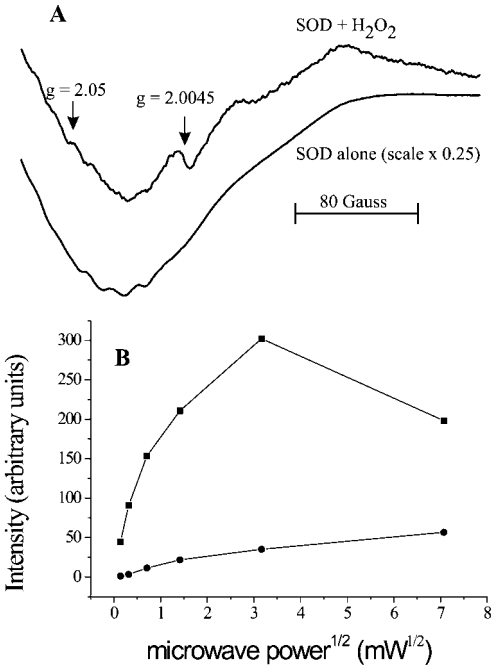

FIG. 8. **Direct EPR spectrum of a frozen solution containing SOD and H_2O_2.** *A*, *upper spectrum*: a solution containing SOD (1 mM Cu) and H_2O_2 (8 mM) was frozen in liquid nitrogen and its EPR spectrum was recorded under liquid nitrogen. The isotropic feature at g = 2.0045 was not observed in the absence of added H_2O_2. The spectrum was obtained using a microwave power of 0.5 mW. *Lower trace*: the EPR spectrum of untreated SOD (1 mM Cu). The difference in intensity between the two spectra likely results from the partial reduction of the active site copper ion from Cu^{2+} to Cu^{+} by the added H_2O_2 (Reaction 4 in the text). *B*, power saturation curve for the lines at g = 2.0045 and g = 2.05. The two lines have distinctly different saturation characteristics, indicating that they are not from the same radical.

detected in the H_2O_2-treated SOD but not the non-treated SOD (not shown). In addition, a line was observed at g = 2.05, which is appropriate for $g_{||}$ of a frozen peroxyl radical. However, the lines at g = 2.05 and g = 2.0045 (possibly corresponding to the $g_{||}$ and $g_{\perp}$ of a peroxyl radical) had different power saturation characteristics (Fig. 8*B*), indicating that they arose from different species, and therefore indicating that the signals did not arise from a peroxyl radical. The line at g = 2.05 and the other small lines observed in both the peroxide-treated and -untreated SOD likely are due to hyperfine couplings from the copper ligands.

DISCUSSION

The spin trapping results strongly support the assignment of the detected MNP/˙SOD radical adduct to a histidinyl radical. A great deal of structural information about the spin-trapped free radical can be obtained from the hyperfine coupling constants obtained from the isotopically labeled histidines. The detected hyperfine coupling to the ^{13}C from the imidazole C-2-labeled histidine provides clear evidence for trapping at that carbon atom (Fig. 2*G* compared with Fig. 2*D*). The nearly identical hyperfine coupling constants to both imidazole nitrogen atoms also supports the assignment to C-2 of the imidazole ring, since they are both one bond away from C-2. Since neither proton hyperfine coupling arose from an exchangeable proton, it is likely that the hydrogen atom giving rise to the larger coupling is bound to C-2 of the imidazole ring (Fig. 9). The other resolved proton hyperfine coupling likely comes from the hydrogen atom at C-5 of the imidazole ring and is likely resolved because of the near-aromatic nature of the imidazole ring.

The primary reaction between HO˙ and histidine has been suggested to be the addition of HO˙ to the imidazole ring,

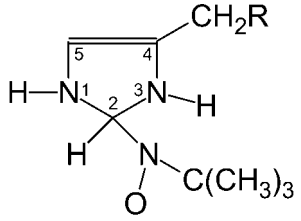

FIG. 9. **The proposed structure of the MNP/˙His radical adduct showing the numbering of the atoms on the imidazole ring.**

primarily at C-2 and C-5 (21–24). The above hyperfine coupling analysis supports trapping a free radical centered at C-2 of the imidazole ring. It has been predicted that addition of HO˙ to C-5 of the imidazole ring would result in a radical with significant electron density at C-2 (21, 22), which could subsequently react with the spin trap to provide the detected adduct. Alternately, the product formed by addition of HO˙ to C-5 of the imidazole ring could dehydrate to produce a free radical with significant electron density at C-2 of the imidazole ring (25). It is unlikely, however, that a free radical resulting from the addition of hydroxyl radical at C-2 of the imidazole ring was trapped. Formation of that radical adduct would require either deprotonation at C-2 after hydroxyl radical addition at that position (unlikely because it would require breaking a σ-bond on what is probably a π-radical) or would result in forming a carbon atom with 5 bonds. It is also possible that the free radical trapped from free histidine (but not necessarily SOD) is the free radical formed by addition of hydroxyl radical to C-5 of the imidazole ring, which has been directly observed both at pH 2 and 7 (21, 24). The resulting hydroxyl addition radical would have to dehydrate to form 2-oxohistidine.

The UV spectrum of the product of the reaction between SOD and H_2O_2 under anaerobic conditions was much more similar to the product of the reaction between free histidine and aqueous electrons than it was to the spectra of the products of the reaction between histidine and HO˙ (22). That result also supports the formation of the histidinyl radical through electron transfer rather than through the addition of hydroxyl radical to the imidazole ring. Electron transfer between different sites on proteins is well established, including reactions that result in free radical formation on amino acid residues remote from the initial site of oxidation (26, 27).

The reactions of the histidinyl radical formed on SOD may be more important than the radical formation itself. In particular, the reactions between carbon-centered free radicals and oxygen to form peroxyl radicals may be responsible for more oxidative damage to cells than all of their other reactions combined. The peroxyl radical formed in the reaction between metmyoglobin and H_2O_2 is capable of oxidizing substrates that are not oxidized by the compound I-like heme intermediate formed in the same reaction (28). The free radical formed in the reaction between free histidine and HO˙ readily reacted with O_2, presumably to form the corresponding peroxyl radical (Fig. 6*A*). The observed oxygen consumption is consistent with previously reported oxygen-dependent changes in the UV-visible spectrum of histidine-HO˙ incubations (22). A histidine peroxyl radical which likely arose from the addition of oxygen to the radical formed by addition of hydroxyl radical at C-5 of the imidazole ring was observed using direct EPR spectroscopy at pH 2 (24). Peroxyl radical formation from the SOD-centered histidinyl radical is also supported by our results (Figs. 5 and 7). The oxygen dependence of 2-oxohistidine formation and the oxygen consumption by incubations containing cuprous SOD and H_2O_2 both indicate formation of an unstable intermediate peroxyl radical. The inhibition of oxygen consumption and of 2-oxohistidine formation by MNP suggests a competition for

the histidinyl radical between the MNP and oxygen. Competition between MNP and O_2 is reasonable due to the 100-fold concentration difference (MNP at 20 mM, O_2 at about 200 μM). Our inability to directly detect the proposed peroxyl radical intermediate could have several causes. First, many peroxyl radicals cannot be detected at temperatures higher than liquid helium temperatures. Second, it is possible that the proposed SOD-peroxyl radical is very unstable and readily decomposes with formation of the corresponding alkoxyl radical (which could then be reduced to form 2-oxohistidine) or some other product, also preventing its detection by direct EPR spectroscopy.

The reaction between SOD and H_2O_2 has received a great deal of attention in recent years due to the well established link between inheritance of a mutant SOD and the development of ALS. An increased peroxidase reaction in the mutant SODs was one of the first mechanisms to be proposed and investigated as a possible molecular cause of the disease (6, 7). More recent results, however, have suggested that the mutant SODs have a similar peroxidase activity to the wild-type protein (3). A role for H_2O_2 in the propagation of ALS disease has been clearly established by the observed protective effects from treatment of transgenic mice expressing a mutant SOD with putrescine-labeled catalase (29).

Because protein-centered free radicals in most cases represent significantly oxidizing centers, the formation of a SOD-centered radical could promote transfer of oxidizing equivalents to other cellular components. Other cellular proteins represent a potential target for $SOD^{\bullet}$-mediated oxidations, since protein-centered radicals have been shown to oxidize other proteins (30) which frequently contain oxidizable centers (cysteine, tyrosine, tryptophan, and histidine residues) that are important to enzyme activities (27). Co-expression of mutant but not wild-type SOD with a glutamate transporter in *Xenopus* oocytes led to the H_2O_2-dependent inactivation of the transporter (31). The inactivation was dependent upon the C-terminal portion of the transporter, which contains many oxidizable amino acid residues (31). Since proteins like the neuronal glutamate transporter frequently have cell-specific functions that are crucial to cellular survival, oxidative damage to those proteins could lead to cell-specific toxicity such as is observed in SOD-linked fALS.

The fALS-associated mutant SODs have also been suggested to cause toxicity through a decreased solubility that leads to the formation of SOD-containing protein aggregates (32–35). The damage to SOD through its self-peroxidation reaction could readily lead to decreased solubility. A conservative mutation to the SOD from *Photobacterium leiognathi* resulted in a zinc-dependent dissociation of the subunits to form inactive monomers (36). Conversion of a histidine residue in SOD to 2-oxohistidine could result in a similar effect. The mutant SODs have been shown to have a reduced zinc affinity compared with the wild-type enzyme *in vitro* (37–39). Conversion of SOD from the native dimer to a monomer could dramatically affect its solubility, particularly when combined with a mutation that also results in some structural destabilization (40).

The reaction between bovine SOD and H_2O_2 or another small organic hydroperoxide resulted in the formation of a histidinyl radical that was spin trapped with MNP. The resulting histidinyl radical reacts with molecular oxygen to form an intermediate peroxyl radical that subsequently decays to form 2-oxohistidine. Further experiments to determine the site(s) of free radical formation in the self-peroxidase reactions of the fALS-associated mutant human SODs might provide information regarding a possible role for the self-peroxidation reaction in the initiation or propagation of motor neuron death in fALS.

REFERENCES

1. Hodgson, E. K., and Fridovich, I. (1975) *Biochemistry* **14,** 5294–5299
2. Hodgson, E. K., and Fridovich, I. (1975) *Biochemistry* **14,** 5299–5303
3. Singh, R. J., Karoui, H., Gunther, M. R., Beckman, J. S., Mason, R. P., and Kalyanaraman, B. (1998) *Proc. Natl. Acad. Sci. U. S. A.* **95,** 6675–6680
4. Sankarapandi, S., and Zweier, J. L. (1999) *J. Biol. Chem.* **274,** 1226–1232
5. Wiedau-Pazos, M., Goto, J. J., Rabizadeh, S., Gralla, E. B., Roe, J. A., Lee, M. K., Valentine, J. S., and Bredesen, D. E. (1996) *Science* **271,** 515–518
6. Yim, H-S., Kang, J-H., Chock, P. B., Stadtman, E. R., and Yim, M. B. (1997) *J. Biol. Chem.* **272,** 8861–8863
7. Lyons, T. J., Liu, H., Goto, J. J., Nersissian, A., Roe, J. A., Graden, J. A., Café, C., Ellerby, L. M., Bredesen, D. E., Gralla, E. B., and Valentine, J. S. (1996) *Proc. Natl. Acad. Sci. U. S. A.* **93,** 12240–12244
8. Ahmed, M. S., Hung, W-Y., Zu, J. S., Hockberger, P., and Siddique, T. (2000) *J. Neurol. Sci.* **176,** 88–94
9. Andrus, P. K., Fleck, T. J., Gurney, M. E., and Hall, E. D. (1998) *J. Neurochem.* **71,** 2041–2048
10. Ferrante, R. J., Shinobu, L. A., Schulz, J. B., Matthews, R. T., Thomas, C. E., Kowall, N. W., Gurney, M. E., and Beal, M. F. (1997) *Ann. Neurol.* **42,** 326–334
11. Liochev, S. I., Chen, L. L., Hallewell, R. A., and Fridovich, I. (1998) *Arch. Biochem. Biophys.* **352,** 237–239
12. Uchida, K., and Kawakishi, S. (1994) *J. Biol. Chem.* **269,** 2405–2410
13. Uchida, K., and Kawakishi, S. (1986) *Biochem. Biophys. Res. Commun.* **138,** 659–665
14. Duling, D. R. (1994) *J. Magnet. Reson. B* **104,** 105–110
15. Bateman, R. C., Jr., and Hersh, L. B. (1987) *Biochemistry* **26,** 4237–4242
16. Makino, K., Suzuki, N., Moriya, F., Rokushika, S., and Hatano, H. (1981) *Radiat. Res.* **86,** 294–310
17. Borders, C. L., Jr., and Fridovich, I. (1985) *Arch. Biochem. Biophys.* **241,** 472–476
18. Lepock, J. R., Arnold, L. D., Torrie, B. H., Andrews, B., and Kruuv, J. (1985) *Arch. Biochem. Biophys.* **241,** 243–251
19. Roe, J. A., Butler, A., Scholler, D. M., Valentine, J. S., Marky, L., and Breslauer, K. J. (1988) *Biochemistry* **27,** 950–958
20. Gunther, M. R., Hanna, P. M., Mason, R. P., and Cohen, M. S. (1995) *Arch. Biochem. Biophys.* **316,** 515–522
21. Lassmann, G., Eriksson, L. A., Lendzian, F., and Lubitz, W. (2000) *J. Phys. Chem. A* **104,** 9144–9152
22. Rao, P. S., Simic, M., and Hayon, E. (1975) *J. Phys. Chem.* **79,** 1260–1263
23. Samuni, A., and Neta, P. (1973) *J. Phys. Chem.* **77,** 1629–1635
24. Lassmann, G., Eriksson, L. A., Himo, F., Lendzian, F., and Lubitz, W. (1999) *J. Phys. Chem. A* **103,** 1283–1290
25. Bansal, K. M., and Sellers, R. M. (1975) *J. Phys. Chem.* **79,** 1775–1779
26. Wilks, A., and Ortiz de Montellano, P. R. (1992) *J. Biol. Chem.* **267,** 8827–8833
27. Hawkins, C. L., and Davies, M. J. (2001) *Biochim. Biophys. Acta* **1504,** 196–219
28. Tschirret-Guth, R. A., and Ortiz de Montellano, P. R. (1996) *Arch. Biochem. Biophys.* **335,** 93–101
29. Reinholz, M. M., Merkle, C. M., and Poduslo, J. F. (1999) *Exp. Neurol.* **159,** 204–216
30. Deterding, L. J., Barr, D. P., Mason, R. P., and Tomer, K. B. (1998) *J. Biol. Chem.* **273,** 12863–12869
31. Trotti, D., Rolfs, A., Danbolt, N. C., Brown R. H., Jr., and Hediger, M. A. (1999) *Nat. Neurosci.* **2,** 427–433
32. Bruijn, L. I., Becher, M. W., Lee, M. K., Anderson, K. L., Jenkins, N. A., Copeland, N. G., Sisodia, S. S., Rothstein, J. D., Borchelt, D. R., Price, D. L., and Cleveland, D. W. (1997) *Neuron* **18,** 327–338
33. Bruijn, L. I., Houseweart, M. K., Kato, S., Anderson, K. L., Anderson, S. D., Ohama, E., Reaume, A. G., Scott, R. W., and Cleveland, D. W. (1998) *Science* **281,** 1851–1854
34. Shibata, N., Hirano, A., Kobayashi, M., Siddique, T., Deng, H-X., Hung, W-Y., Kato, T., and Asayama, K. (1996) *J. Neuropathol. Exp. Neurol.* **55,** 481–490
35. Kato, S., Shimoda, M., Watanabe, Y., Nakashima, K., Takahashi, K., and Ohama, E. (1996) *J. Neuropathol. Exp. Neurol.* **55,** 1089–1101
36. D'Orazio, M., Battistoni, A., Stroppolo, M. E., and Desideri, A. (2000) *Biochem. Biophys. Res. Commun.* **272,** 81–83
37. Crow, J. P., Sampson, J. B., Zhuang, Y., Thompson, J. A., and Beckman, J. S. (1997) *J. Neurochem.* **69,** 1936–1944
38. Goto, J. J., Zhu, H., Sanchez, R. J., Nersissian, A., Gralla, E. B., Valentine, J. S., and Cabelli, D. E. (2000) *J. Biol. Chem.* **275,** 1007–1014
39. Estevez, A. G., Crow, J. P., Sampson, J. B., Reiter, C., Zhuang, Y., Richardson, G. J., Tarpey, M. M., Barbeito, L., and Beckman, J. S. (1999) *Science* **286,** 2498–2500
40. Deng, H-X., Hentati, A., Tainer, J. A., Iqbal, Z., Cayabyab, A., Hung, W-Y., Getzoff, E. D., Hu, P., Herzfeldt, B., Roos, R. P., Warner, C., Deng, G., Soriano, E., Smyth, C., Parge, H. E., Ahmed, A., Roses, A. D., Hallewell, R. A., Pericak-Vance, M. A., and Siddique, T. (1993) *Science* **261,** 1047–1051